Available online at www.sciencedirect.com
ScienceDirect
International Journal of Mass Spectrometry 269 (2008) 71–77
International Journal of Mass Spectrometry
www.elsevier.com/locate/ijms

Absolute measurements of isotope amount ratios on gases Part II. Application of the measurement models developed on real gases

S. Valkiers [a,*], M. Varlam [a], M. Berglund [a], P. Taylor [a], R. Gonfiantini [b], P. De Bièvre [c]

[a] *Institute for Reference Materials and Measurements, EC-JRC, 2440 Geel (B), Belgium*
[b] *Istituto di Geoscienze e Georisorse, Via G. Moruzzi 1, 56124 Pisa (I), Belgium*
[c] *Independent Consultant on Metrology in Chemistry, Duineneind 9, 2460 Kasterlee (B), Belgium*

Received 17 July 2007; received in revised form 17 September 2007; accepted 17 September 2007
Available online 5 October 2007

Abstract

The power of the theoretical formalisms based on concepts from kinetic gas theory described in Part I of this series, is demonstrated in isotope measurement results obtained for three different gases: CO_2, SiF_4 gas highly enriched in the ^{28}Si isotope and a high purity neon gas of natural isotopic composition. The measurement procedure as described in this paper enables to detect various (small) anomalies in the gas mass spectrometer during the ion current measurements thus creating the opportunity to correct for them.

Using these concepts which govern the isotope fractionation of the gas in the mass spectrometer and performing a calibration by means of synthesized values for isotope amount ratios, SI traceable values in terms of the derived measurement unit mol/mol can be obtained.

Keywords: Isotope ratio mass spectrometry; Kinetic gas theory; Absolute isotope amount ratio; SI-traceability

1. Introduction

The strategy underlying 'absolute' isotope amount ratio measurements, are basically different from those underlying "δ-measurements". Instead of being concentrated to ensure "identical conditions" in the mass spectrometer (for reference and sample), the approach is to maximize, but know and control the isotope fractionation process in the molecular gas flow from the inlet system to the ion source. The basic processes that take place are similar to those in any other commercial gas IRMS-electron impact ionization, the formation and focusing of ion beams in the source, the magnetic deflection and the detection (Faraday/with the subsequent Secondary Electron Multiplier), but the strategy is to use the known dynamics of the gas flow in the ion source and of the measured ion currents when produced under very stable and known conditions.

The theoretical concepts underlying measurements of 'absolute' isotope amount ratio values on gases have been described in Part I of this series [1], where the mathematical and physical backgrounds which underpin this kind of "absolute" measurement procedure are presented and discussed.

The theoretical treatment [1] of the data which is the *keystone* of this type of measurements is based on basic physical principles and only a few assumptions must be taken into account with small effects. This approach is different from differential measurements (δ-measurements) not only by its approach but also by the nature of the results: "absolute" isotope amount ratios are obtained.

The measurement equations used in performing isotope amount ratio measurements ("IARM") [1] describe a transparent and traceable relationship between an isotope amount ratio of an element (the quantity intended to be measured, i.e., the 'measurand') in a specific sample in the measurement unit mol/mol, to its measured ion current ratio (the quantity subject to measurement), as measured in A/A.

2. Measurements of isotope amount ratios on gases

The isotope amount ratio measurements in this work are performed on the 'Avogadro II amount comparator' [2–5], a gradually modified MAT271 isotope gas mass spectrometer [6–11], measuring ion current ratios. The measurements are

* Corresponding author. Tel.: +32 14 571 639; fax: +32 14 571 863.
E-mail address: staf.valkiers@ec.europa.eu (S. Valkiers).

1387-3806/$ – see front matter © 2007 Elsevier B.V. All rights reserved.
doi:10.1016/j.ijms.2007.09.019

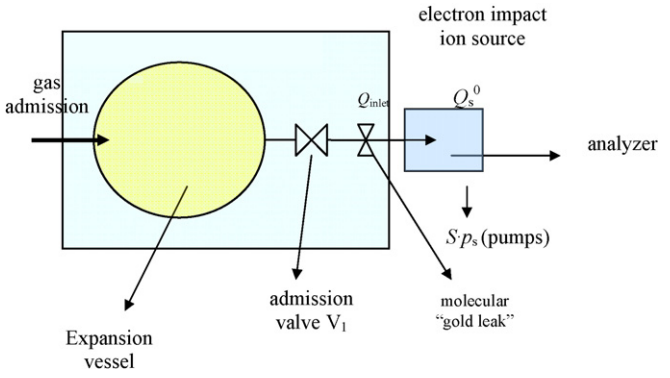

Fig. 1. Gas inlet system of the MAT271 gas mass spectrometer.

monitored sequentially using one Faraday cup (with different amplification channels) and one SEM/ion detector positioned at the required mass-to-charge positions in the mass spectrum. Short-term fluctuations of the ion currents are eliminated by performing a symmetrical scanning [8,9] over the peaks. As usual, the observed ion current ratios $J_{i/j}$ must be converted into isotope amount ratios R_{true}. The correction factors $K = R_{i/j}/J_{i/j}$ are expected to be close to unity. They are obtained by measuring synthesized amount ratios with $R_{i/j}$ is generated from the preparation of synthetic isotope mixtures [6,7].

During the measurement, the sample in the expansion vessel of the spectrometer changes in isotopic composition over time because of the effusion out of the expansion vessel through the gold foil to the inlet of the spectrometer (Fig. 1). It is molecular mass dependent [1,11,12]. Extrapolation of the measured ion current ratios over time to the start of the measurement ($t = 0$), is required to determine the initial isotopic composition of the element in the sample. One of the most sensitive parameters in such measurements is the gas flow (with its associated physical and chemical) processes as it interacts with the inlet system surface of the mass spectrometer. Ultra-high precision ion current ratio measurements are very well suited for studying effects related to adsorption/desorption processes in the inlet system of the mass spectrometer and for isotope exchange reactions at surfaces [11,12]. Also synthetic isotope mixtures are excellent means to study and measure these effects. They should be reliable and transparent [6,7]. Thus, different sources of measurement uncertainties can be easily identified in a step-by-step breakdown and, as a result, isotope amount ratios can be obtained with known and very small combined uncertainties. Such an approach leads to the selection of particular types of methods and instrumentation which are different from what researchers use in 'differential' measurements.

3. Applications of the kinetic gas models to real gases

3.1. Applying the model on isotope amount ratio measurements in CO_2

As a first demonstration of the power of the mathematical model developed [1], measurements were made on CO_2 gas of natural isotopic composition [2–4]. CO_2 is a complex gas because of its large number of isotopomers of the molecule, which in turn can be used as an advantage.

Isotope amount ratio measurements by differential mass spectrometry on CO_2 are usually performed only at positions 44, 45 and 46 in the mass spectrum. They provide insufficient information for the determination of isotope amount fractions for carbon and oxygen. However, supplementary ion current ratio measurements $J_{47/44} = I[^{47}(CO_2)^+]/I[^{44}(CO_2)^+]$ are required. They are difficult to perform [2–4], as the size of the ion current ratio $J_{47/44}$ is in the 10^{-5} range. Common mass spectrometers are limited by their dynamic measurement range to measure them. Hence, the modified MAT271 gas mass spectrometer [8–10] used in this work is the result of a continuous further development leading to the ability to perform measurements of small ion currents down to 1 fA. For the CO_2 gas a measurement sequence has been set up for the ion current ratios $J_{i/44} = I[^{i}(CO_2)^+]/I[^{44}(CO_2)^+]$ with $i = 45$–47, enabling to determine afterwards the fractional abundances for the carbon and oxygen isotopes [5]. The relationship between the amount of CO_2 gas present in the vessel (Fig. 1) and its ion currents $I[^{i}(CO_2)^+]$ measured, with $i = 44$–47, can be obtained [1] via Eq. (1):

$$\frac{T_s}{\varepsilon_{eff}}\frac{d(I - I_{backg})}{dt} = \frac{C_0}{V_{inlet}}T_{inlet}\sqrt{\frac{T_{inlet}}{M}}(n_{inlet} - n_{bg\,inlet}) - \frac{S}{V_s}\frac{T_s}{\varepsilon_{eff}}(I - I_{backg}) \quad (1)$$

The majority of pumping systems are operating at molecular flow conditions and have pumping speeds S (Eq. (2)) which are obeying the Knudsen law, proportional to $\sqrt{1/M}$ and to the temperature of the gas; this is similar for turbo-molecular pumping systems [1]:

$$S = S_o\sqrt{\frac{1}{M}} \quad (2)$$

S_o is the constant for a pressure range varying from 10^{-3} to 10^{-7} Pa. However, it is determined by the diameter of the flange at the pump (Fig. 1).

Introducing Eq. (2) in Eq. (1), and transforming it into a logarithmic equation yields [1]:

$$\ln\left[\frac{d(I - I_{backg})t}{dt} + \frac{S_o}{V_s}\frac{1}{\sqrt{M}}(I - I_{backg})t\right] = \ln\left[\frac{d(I - I_{backg})_0}{dt} + \frac{S_o}{V_s}\frac{1}{\sqrt{M}}(I - I_{backg})_0\right]_o - \frac{\sqrt{T_{inlet}}C_o}{V_{inlet}\sqrt{M}}t \quad (3)$$

This logarithmic function of the type ($\ln I = \ln I_0 - bt$) (Eq. (3)), is valid for each ion current measured by the MAT271, with b being the slope of the line and depending on the molar mass of the isotopomer concerned. The other parameters involved in Eq. (3) are constants for given measuring conditions (in the inlet and ion source) of the mass spectrometer. Any deviation

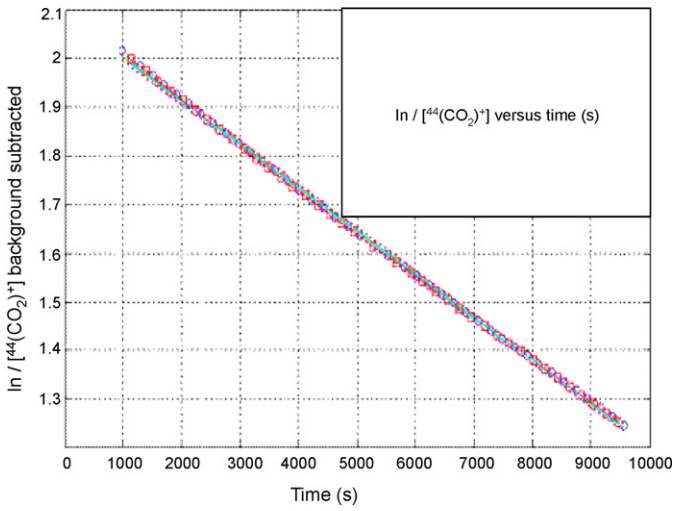

Fig. 2. A logarithmic presentation of the ion current $I[^{44}(CO_2)^+] \times 10^{-10}$ A vs. time (in s) measured on CO_2 gas of a natural carbon and oxygen isotopic composition. The squared points are values obtained by using Eq. (3). In the other treatment the dynamic part is neglected (i.e., only values for $\ln I[^{44}(CO_2)^+]$ vs. time are displayed).

from this relationship (Eq. (3)) is a qualitative indicator that the experimental conditions for attaining ideal gas behavior are not completely fulfilled.

The term $d(I - I_{backg})t/dt$ in Eq. (3) constitutes a small correction of the deviation from the steady-state condition in the ion source and the inlet vessel. Its effect is only of importance in some special cases such as in measurements of very small ion currents.

In Fig. 2 the relationship ion current $I[^{44}(CO_2)^+]$ versus time measured on CO_2 gas is visualized with the decrease of the ion current treated in two different ways. The small circles show the ion currents that are treated according to Eq. (3). They use the previously determined [1] value for S_o/V_s, while in the other treatment (squares) the dynamic part is neglected.

When absolute isotope amount ratio values are the target, then Fig. 2 has no practical meaning. It is only a powerful tool to check any occurrence (even if extremely small) of a viscous character of the molecular gas flow to the ion source [2,3]. For a typical measurement as shown in Fig. 2, the uncertainty on the slope is of the order of 10^{-5} relative or better.

When applying Eq. (3), it was demonstrated that this slope is indeed proportional to the square root of the molar mass of the isotopomer measured: its proportionality constant is depending only on the geometry of the mass spectrometer and of the temperature of the inlet vessel ($\sqrt{T_{inlet}}C_o/V_{inlet}$). Hence, considering that the temperature is constant (±0.01 °C) over the entire scan (up to 5000 s), the *ratio* of two of such slopes (for different m/z values) has to be equal to the square root of their mass-to-charge ratios. In Table 1 the slopes of $I[^i(CO_2)^+]$ versus time are shown, with their measurement uncertainties. These are dependent from small variations of the temperature in the ion source and in the inlet system vessel (which directly affect the molecular gas flow).

As demonstrated by Eq. (3), the slope values b (Table 1) obtained on CO_2, are indeed proportional to the molar mass of

Table 1
Values ($b = \sqrt{T_{inlet}}C_o/V_{inlet}\sqrt{M}$) of the function $\ln y = \ln y_0 - bt$ for the linear regression of the measured ion currents $I[^i(CO_2)^+]$, with $i = 44$–47 on natural CO_2 gas as mean value of about 20 measurements, performed over about 2 months of time

Mass-to-charge ratio for measurements of the ion current $I[^i(CO_2)^+]$, with $i = 44$–47	$b = (\sqrt{T_{inlet}}C_o/V_{inlet}\sqrt{M}) \times 10^{-4}$
44	9.454 32 (85)
45	9.360 2 (10)
46	9.278 91 (92)
47	9.203 4 (75)

the measured isotopomer (Fig. 2). The small deviations from their linear behavior are caused by the (inevitable) small temperature instabilities at the inlet system; a deviation of 0.1 °C generates already a deviation of $\sim 10^{-6}$ rel. on the slope. However, this does not matter too much as *ratios of ion currents* are used.

The data as shown in Fig. 2 is corrected for background as obtained via measurements with the inlet vessel empty (with admission valve V_1 open in Fig. 1). The ion current values I_{backg} as required for Eq. (3) were measured in the combined Faraday and SEM/ion counting mode because of their small size. A typical background measurement $I[^{44}(CO_2)^+]$ versus time (t/s) is shown in Fig. 3; it is caused by the remainder of pumping and desorption processes. Any further systematic deviations from the regression as presented in Fig. 2 could be seen as possible instabilities related to the sample: (a) isotopic non-equilibrium, or (b) caused by other processes in the ion source, like ion-molecule reactions.

In Table 1 such a deviation from linearity can be observed. Most probably, it is created by additional reactions which took place in the ion source. However, when applying Eq. (3), the linear regression to time $t = 0$, yields the isotopic composition of the original gas (free of any isotope fractionation during sample inlet in the spectrometer).

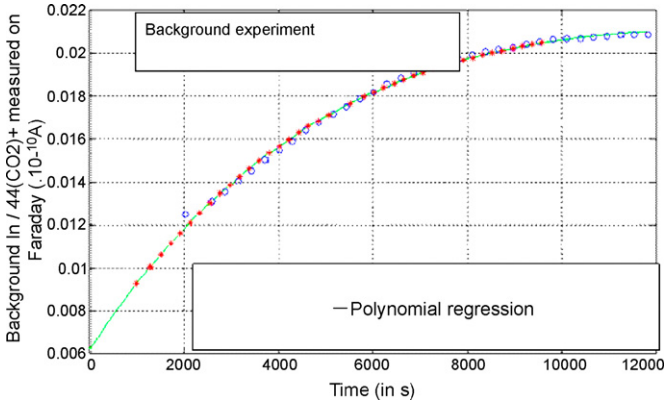

Fig. 3. The measured ion current $I[^{44}(CO_2)^+]$ vs. time (in s) measured at $m/z = 44$, obtained with an empty inlet vessel and admission valve V_1 opened, see Fig. 1. These background values are obtained via measurements with the detection system in Faraday and SEM/ion counting mode (because of the small size of the ion currents) operated in simultaneous mode within the detection system.

The variation of isotope amount *ratio* with time [1] for a gas consisting of two isotopes (and applying Eq. (3)) can now be given as

$$\ln\left\{\sqrt{\frac{M_2}{M_1}}\,\frac{(\mathrm{d}(I_2(t)-I^{\mathrm{backg}}(t))/\mathrm{d}t)+(S_\mathrm{o}/V_\mathrm{s})(1/\sqrt{M_2})[I_2(t)-I^{\mathrm{backg}}(t)]}{(\mathrm{d}(I_1(t)-I^{\mathrm{backg}}(t))/\mathrm{d}t)+(S_\mathrm{o}/V_\mathrm{s})(1/\sqrt{M_1})[I_1(t)-I^{\mathrm{backg}}(t)]}\right\}=\ln[R^{\mathrm{o}}_{\mathrm{inlet}}]+\left[\frac{C_\mathrm{o}\sqrt{T_{\mathrm{inlet}}}}{V_{\mathrm{inlet}}}\left(\frac{1}{\sqrt{M_1}}-\frac{1}{\sqrt{M_2}}\right)\right]t \quad (4)$$

As indicated already, the detection system of MAT271 enables to measure ion currents over a 10^7 range (1 fA to 10 μA). On natural CO_2 ion currents, $I[^i(CO_2)^+]$ with $i=44$–49 could be measured in one experiment. To perform the ion current ratio measurements $I[^i(CO_2)^+]/I[^{44}(CO_2)^+]$ ($i=45$–49) on natural CO_2, the entire detection system of the MAT271 is needed: Faraday detection with a 3×10^9 high ohmic resistor, Faraday detection with a 3×10^{11} high ohmic resistor and, in order to be able to measure the smallest ion currents, a Secondary Electron Multiplier in ion counting mode, with a dynamic calibration connecting both amplification systems. To avoid any drift of the calibration factor (caused by temperature variations of the amplifiers within the amplifier house), the currents obtained via both amplification systems are continuously measured throughout the measurement, and ion currents dynamically linked to the same Faraday detector (with lowest amplification) in order to be able to 'trace' calculated ratios to the same reference. In Fig. 4 the calibrations factors are visualized.

As ion currents are measured over a large dynamic range by the instrument, its linearity over time is of crucial importance because a single measurement could take up to 5 h. To demonstrate this linearity, a measurement of the ion current $I[^{44}(CO_2)^+]$ was made over 12 h. The measurement uncertainty calculated on the linearity fit was of the order of 10^{-5} relative.

Obviously the measurements as shown in Fig. 2 are basic data treatments for the measured ion currents which result from ionization of only one unique isotopomer. When however several isotopomers are effusing from the inlet vessel, this regression clearly will show a visible deviation from linearity. This deviation could be of practical importance in quantifying some other small corrections (by assuming that all the contributors are clearly known). Furthermore, when ion-molecule reactions are involved (suggested by a deviation from linearity) a mathematical solution can be found using such measured data.

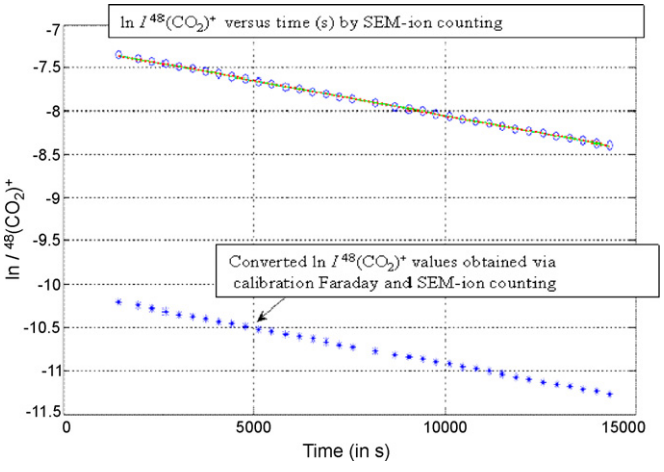

Fig. 4. A logarithmic presentation of the ion current $I[^{48}(CO_2)^+]$ vs. time (in s) measured on CO_2 gas with a natural carbon and oxygen isotopic composition. The measurement was made in SEM/ion counting mode, and via the previously determined conversion factor SEM/Faraday the ion counting signal could be compared to the one which was measured on Faraday (with a 3×10^{11} high ohmic amplification).

The purpose of the data treatment developed in this paper is to arrive at 'absolute' isotope amount ratios of the sample as introduced into the inlet vessel. Therefore, using Eq. (4) with a linear least-square regression of the measured data (for two different isotopomers), will provide the extrapolated ratio at time $t=0$.

The slope of this linear regression is dependent from the molar mass values of the two isotopomers involved. The proportionality constant between the slope value and molar masses is an instrumental factor with constant value and is taken as a quantitative indicator of the accuracy of the measurement result for a specified isotope amount ratio.

The final calibration of the MAT271 mass spectrometer is made with the help of synthesized amount ratio values within mixtures of enriched isotopes; a comprehensive description of this calibration as exemplified for CO_2 is given in [2–5]. The correction factors K thus obtained, will 'correct' the observed isotope amount ratios for systematic effects and deviations from the assumptions in the mathematical model. The closer the K-values are to unity, the smaller the deviations will be from the values assumed in the model.

3.2. Applying the model on isotope amount ratio measurements in SiF_4 of nearly pure $^{28}SiF_4$

A further attempt to reduce the measurement uncertainty of the Si molar mass value (and hence the Avogadro constant) has been started up in 2004 by fabricating two Si single crystal spheres of ≥99.99% enriched ^{28}Si [13–16], which means ^{29}Si and ^{30}Si minor isotope abundances of the order of 0.005%. A relative combined uncertainty of ≤1% on each of these abundance values contributes a relative uncertainty on the molar mass of the Si of $\leq3\times10^{-8}$. For the molar mass values that means that the calibrated measurement of the isotope amount ratios of Si of *natural* isotopic composition using synthetic isotope mixtures can be replaced by the measurement of (very) small ^{29}Si and ^{30}Si isotope abundances in the highly enriched ^{28}Si (Fig. 5). That results in small corrections to the molar mass value of the pure ^{28}Si, known to a relative combined uncertainty of $\leq10^{-9}$. As these corrections will be measured, only the uncertainty of these (very) small corrections will enter in the total uncertainty budget of the molar mass of the Si in the highly enriched ^{28}Si in the Avogadro crystal. These isotope amount ratio are performed by measuring the ion current ratios $J_{i/28}=I[(^i\mathrm{SiF_3})^+]/I[(^{28}\mathrm{SiF_3})^+]$, with $i=29$ and 30 on SiF_4 gas [1,15,16].

Such ion current ratio measurements are monitored sequentially using one Faraday cup with signals amplified over two high

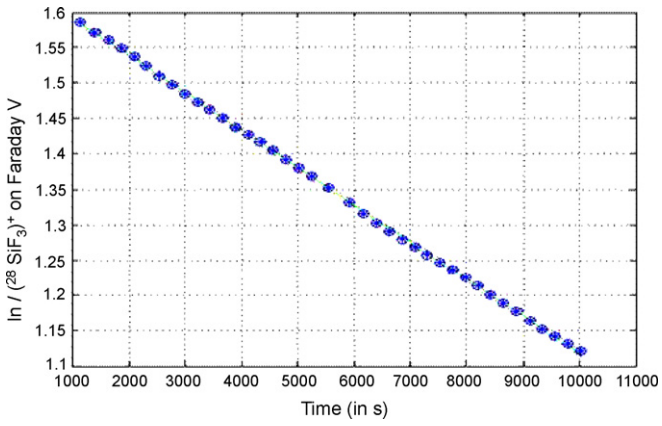

Fig. 5. Visualisation of the logarithm of the ion current $I[(^{28}SiF_3)^+]$ vs. time (in s) measured on a 99.99% isotopically enriched $^{28}SiF_4$ sample (code Si28-7.2.1/Avogadro) with the data as treated by Eq. (3).

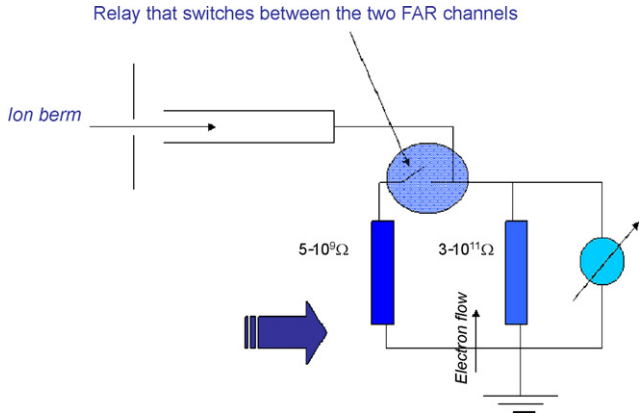

Fig. 6. The detector system of the MAT271 gas mass spectrometer: Faraday detection with a 3×10^9 high ohmic resistor, Faraday detection with a 3×10^{11} high ohmic and, in order to be able to measure the smallest ion currents a Secondary Electron Multiplier for ion counting.

Ohmic resistors (3×10^9 Ω for $I[(^{28}SiF_3)^+]$ and 3×10^{11} Ω for $I[(^{29}SiF_3)^+]$ and $I[(^{30}SiF_3)^+]$) positioned for $m/z = 85$–87, and for $m/z = 104$ as link for the two amplification chains. Measurements on the SEM/ion counting mode are needed (Fig. 6) to decrease the measurement uncertainty of the ion current ratios significantly (as compared for instance to CO_2 measurements). Short-term fluctuations are eliminated by symmetrically scanning the peaks. In the ideal case, the measured ion current ratios J can be converted directly into isotope amount ratios R. Each ion current ratio measurement takes about 2 h, and mean ion current ratios of at least five successive measurements are obtained, with associated standard deviations (1 s).

Table 2
Values b (or $\sqrt{T_{inlet}}C_o/V_{inlet}\sqrt{M}$) in the function $\ln y = \ln y_0 - bt$ for the linear regression of the measured ion currents $I[(^iSiF_3)^+]$, with $i = 28$–30

Mass-to-charge ratio for measurements of $I[(^iSiF_3)^+]$ with $i = 85$ to 87	$b = (\sqrt{T_{inlet}}C_o/V_{inlet}\sqrt{M}) \times 10^{-5}$ – value $\times 10^{-5}$
85	5.165 32 (45)
86	4.860 2 (25)
87	4.446 3 (95)

On the 99.99% enriched $^{28}SiF_4$ sample (sample code Si28-7.2.1) the logarithm of the ion current, $\ln I[(^{28}SiF_3)^+]$ versus time is shown in Fig. 5 as treated via Eq. (3). From this graph and from measurements of $I[(^{29}SiF_3)^+]$ and $I[(^{30}SiF_3)^+]$ the slopes of the function with their measurement uncertainties were calculated (Table 3).

The values b (Table 2) obtained on 99.99% enriched $^{28}SiF_4$ sample (sample code Si28-7.2.1) are again proportional to the molar mass of the measured isotopomer ($^iSiF_4$). The small deviations from linearity in this specific case are mainly due to the small magnitudes (a few fA) of the measured ion currents $I[(^{29}SiF_3)^+]$ and $I[(^{30}SiF_3)^+]$.

Using Eq. (4) with a least-squares regression [1] of the measured data for the ion current ratios $J_{i/28} = I[(^iSiF_3)^+]/I[(^{28}SiF_3)^+]$, with $i = 29$ and 30, will give their extrapolated value at time $t = 0$.

When data treatment is compared to a simple least square fit, neglecting the dynamic part of Eq. (4), small but significant discrepancies can be observed in the ion current ratios as indicated in Table 3; the effect is small but it needs to be taken into account. Further the treatment by Eq. (4) results in slightly smaller measurement uncertainties (Table 3) on the isotope amount ratio values.

3.3. Applying the model for isotope amount ratio measurements on neon

Less complex are the isotope amount ratio measurements performed on high purity Ne of natural isotopic composition. Neon on Earth is predominately of two different origins: air (which is by far the most common source of commercial neon) and crustal neon (as found in natural gas wells). The internationally recognised value for the isotopic composition of neon (90.92, 0.26 and 8.82 amount % for ^iNe with $i = 20$–22, respectively) is in fact based on isotope measurements of neon in air [18]. Since the neon isotopic composition affects some of the properties of neon relevant to thermometry (i.e., the value of the

Table 3
Results of the logarithmic extrapolation [1] to the start (time $t = 0$) of the ion current ratio measurements $I[(^iSiF_3)^+]/I[(^{28}SiF_3)^+]$ (with $i = 29$ and 30) vs. time (s) measured on highly enriched $^{28}SiF_4$ gas, according to Eq. (4) and by neglecting the dynamic part in the equation (i.e., only considering values for $\ln I[(^iSiF_3)^+]/I[(^{28}SiF_3)^+]$ vs. time)

	Data treatment according to Eq. (4)	Simple least square fit of the data (i.e., the dynamic part is neglected)
$I[(^{29}SiF_3)^+]/I[(^{28}SiF_3)^+]_{t=0}$	0.000 102 414 (51)	0.000 102 419 (61)
$I[(^{30}SiF_3)^+]/I[(^{28}SiF_3)^+]_{t=0}$	0.000 031 795 (25)	0.000 031 790 (35)

The measurement uncertainties (1 s) are standard deviations for five complete independent measurements.

triple point), its isotopic composition needs to be specified for a thermometric standard [3,17,20]. Consequently, a worldwide study is on its way since 2003 concerning the variability of the isotopic composition of commercially available neon, initially in the frame of the European Research Project MULTICELLS, later in the frame of a EUROMET Project, now merged in a Joint Research Project as the European Project iMERA [20]. It is especially directed to the neon samples used in the international inter-comparisons of the isotopic composition from 1978 onwards.

Different neon samples from various commercial suppliers and various batches were supplied to IRMM for a recent study [17] in the realisation of the temperature standards at INRIM[1], LNE-INM, NIST and NMIJ/AIST. All measurements were linked to an IRMM internal standard (commercial high purity neon) leading to the possibility that in this way all future measurement results of neon isotopes (on the same or on other samples) can be linked via this standard, i.e., are made 'comparable' because 'traceable to a common reference' [19]. Present data can only be given as neon *ion current* ratios which are approximately equivalent to their isotope amount ratios. But no corrections for (minor) systematic unknown effects are yet made, because no synthetic isotope mixtures (Primary Measurement Standards) of enriched Ne isotopes are available. Anyhow these corrections will be of the order of 10^{-4} relative (or lower) for the neon isotope amount ratios.

In order to detect small variations in the natural neon isotopes, measurements were made at IRMM on the MAT271 by applying the data treatment as discussed in detail in this paper. Fig. 7 displays the measured ^{22}Ne ion current $I[^{22}(Ne)^+]$ on a high purity neon sample (Carbagas, CH) shown over about 4 h, with the data treated according to Eq. (3) and by applying the earlier determined value for S_o/V_s [1]. The measurement uncertainty calculated on the linear fit (Fig. 7) is again of the order of 10^{-5} relative. By subsequently using Eq. (4) with a linear least-square regression of the measured data, the extrapolated ratios for the neon sample to time $t = 0$ (original isotopic composition of the sample) can be obtained. For the measured ion current ratio $I[^{21}(Ne)^+]/I[^{20}(Ne)^+]$ and $I[^{22}(Ne)^+]/I[^{20}(Ne)^+]$ such linear regression is shown in Fig. 8. An overview of the different neon samples recently measured is given in Table 4.

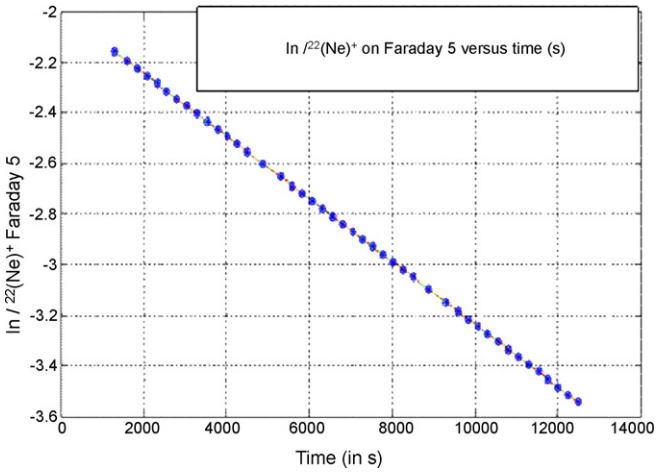

Fig. 7. Visualisation of the ion current $\ln I[^{22}(Ne)^+]$ vs. time (in s), measured on a high purity neon of natural isotopic composition (Carbagas, CH) with the data as treated by Eq. (3).

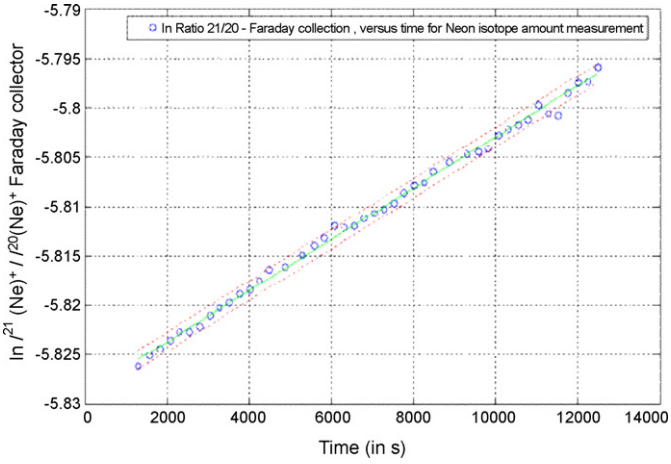

Fig. 8. Least-squares regression of the measured of ion current ratio $J_{21/20} = I[^{21}(Ne)^+]/I[^{20}(Ne)^+]$ vs. time to calculate the intercept $\{I[^{21}(Ne)^+]/I[^{20}(Ne)^+]\}$ at time $t = 0$ (i.e., the isotopic composition of the sample at the sample inlet [1]).

Neon ion current ratios and molar mass values obtained by using Eq. (4) with a linear least-square regression of the measured data (Table 4) and the extrapolated ratios for the neon sample to time $t = 0$ (original isotopic composition of

Table 4
Neon ion current ratios and molar mass values obtained by using Eq. (4) with a linear least-square regression of the measured data and the extrapolated ratios for the neon sample to time $t = 0$ (original isotopic composition of the sample)

	Ion current ratio $I[^{22}(Ne)^+]/I[^{20}(Ne)^+]_{t=0}$	Ion current ratio $I[^{21}(Ne)^+]/I[^{20}(Ne)^+]_{t=0}$	Non-calibrated molar mass M(Ne)
INRIM	0.104 133 2 (44)	0.002 966 42 (51)	20.183 143 1 (72)
Carbagas	0.102 336 6 (34)	0.002 942 47 (74)	20.180 186 3 (56)
Matheson	0.104 797 7 (77)	0.002 975 47 (73)	20.184 234 (12)
NBS-IRM	0.101 797 1 (66)	0.002 931 79 (65)	20.179 294 (10)
INRIM-Matheson	0.103 186 4 (32)	0.002 954 19 (78)	20.181 586 4 (53)
NIST-Airgas	0.103 989 7 (51)	0.002 959 26 (46)	20.182 903 5 (83)
Ne-Air	0.101 975 2 (23)	0.002 937 71 (74)	20.179 590 4 (38)
Ne-Japan-DO74	0.102 250 9 (83)	0.002 939 14 (94)	20.180 043 (13)
Ne-Japan-DO24	0.102 424 1 (74)	0.002 941 28 (77)	20.180 329 (12)

The repeatabilities are given in parentheses as 1 s (applicable to the last two digits of the value). These measurement results cannot be compared with *other* measurement results for the same sample because of the absence, as yet, of a commonly agreed "stated metrological reference" for their metrological traceability.

the sample). The repeatabilities are given in parentheses as 1 s (applicable to the last two digits of the value). These measurement results cannot be compared with *other* measurement results for the same sample because of the absence, as yet, of a commonly agreed "stated metrological reference" for their metrological traceability.

4. Conclusion

When applying isotope fractionation during mass spectrometric measurements of a gaseous sample (consisting of several isotopes) and verified by a "calibration" through synthetic isotope mixtures (primary measurement standards), SI-traceable isotope amount ratio values (in terms of mol/mol) can be obtained. The entire theoretical treatment of the measured data which is the keystone in this type of measurement and based on pure physical principles with only a few minor assumptions, needed to be taken into account [1].

In order to demonstrate the robustness of this measurement procedure and at the same time proving that the measured values are consistent with kinetic gas theory, different ion current ratio measurements were performed on various (multi) isotopic gases (CO_2, SiF_4, Ne). The creation of pure molecular flow conditions of the gaseous sample in the mass spectrometer (and continuously checking the pureness of the molecular flow [3]) results in a predictable mass discrimination at the point of effusion of the gas into the spectrometer (electron impact) ion source. By applying this procedure [1], it is possible to identify and to quantify the uncertainty contributions of the K factor (the factor relating measured ion current ratios to isotope amount-of-substance ratios) and leaving a small 'residual' factor K which can be determined by means of synthetically prepared synthetic mixtures (of enriched isotopes). The amount ratio values in these mixtures are 'synthesized' and measured using the same procedure [1]. These 'synthesized' values are traceable to the definition of the derived unit mol/mol within the International System of Units (SI).

References

[1] M. Varlam, S. Valkiers, M. Berglund, R. Gonfiantini, P. Taylor, P. De Bièvre, Int. J. Mass Spectr. 269 (2007) 78–84.
[2] S. Valkiers, M. Varlam, H. Kuehnm, EUR report 2007, P6506.
[3] S. Valkiers, M. Varlam, M. Berglund, P. Taylor, EUR report 2006, P22509.
[4] S. Valkiers, M. Varlam, K. Ruße, M. Berglund, P. Taylor, J. Wang, M. Milton, P. De Bièvre, Int. J. Mass Spectr. 263 (2007) 195.
[5] S. Valkiers, M. Varlam, K. Ruße, M. Berglund, P. Taylor, J. Wang, M. Milton, P. De Bièvre, Int. J. Mass Spectr. 264 (2007) 10.
[6] P. De Bièvre, G. Lenaers, T. Murphy, S. Valkiers, S. Peiser, Metrologia 32 (1995) 103.
[7] P. De Bièvre, S. Valkiers, P. Taylor, Fresenius J. Anal. Chem. 361 (1998) 227.
[8] S. Valkiers, Y. Aregbe, P. De Bièvre, Int. J. Mass Spectr. Ion Proc. 173 (1998) 55.
[9] S. Valkiers, H. Kipphardt, T. Ding, K. Mayer, P. Taylor, Int. J. Mass Spectr. Ion Proc. 193 (1999) 1.
[10] T.J. Milton, J. Wang, Int. J. Mass Spectr. 218 (2002) 63.
[11] R. Gonfiantini, S. Valkiers, P. De Bièvre, P. Taylor, IEEE Trans. Instrum. Meas. 46 (1997) 566.
[12] R. Gonfiantini, S. Valkiers, P. De Bièvre, Int. J. Mass Spectr. Ion Proc. 161 (1997) 15.
[13] K. Fujii, A. Waseda, N. Kuramoto, S. Mitzushima, P. Becker, H. Bettin, A. Nicolaus, U. Kuetgens, S. Valkiers, P. Taylor, P. De Bièvre, G. Mana, E. Massa, E. Matyi, E. Kessler, IEEE Trans. Instrum. Meas. 84 (2005) 854.
[14] P. Becker, H. Bettin, H.-U. Danzebrink, M. Gläser, U. Kuetgens, A. Nicolaus, D. Schiel, P. De Bièvre, S. Valkiers, P. Taylor, Metrologia 40 (2003) 271.
[15] I. Busch, S. Valkiers, P. Becker, 13th Metrology Congress Lille (F), June 2007.
[16] P. Becker, D. Schiel, H.-J. Pohl, A. Kaliteevski, O. Godisov, M. Churbanov, G. Devyatykh, A. Gusev, A. Bulanov, S. Adamchik, V. Gavva, I. Kovalev, N. Abrosimov, B. Hallmann-Seiffert, H. Riemann, S. Valkiers, P. Taylor, P. De Bièvre, E. Dianov, Meas. Sci. Technol. 17 (2006) 1854.
[17] F. Pavese, B. Fellmuth, D. Head, Y. Hermier, K. Hill, S. Valkiers, Anal. Chem. 77 (15) (2005) 5076.
[18] M. Groening, K. Froehlich, P. De Regge, P. Danesi, Intended use of the IAEA reference materials. Part II. Examples on reference materials for stable isotope composition, Roy. Soc. Chem. 238 (1999) 81.
[19] BIPM, IEC, IFCC, ILAC, ISO, IUPAC, IUPAP, OIML, The International Vocabulary of Metrology—Basic and General concepts and associated Terms (VIM) ISO 99, ISO Geneva, 2007.
[20] http://www.euromet.org/projects/iMERA.